Published for SISSA by Springer

Received: October 9, 2020
Revised: March 25, 2021
Accepted: April 6, 2021
Published: April 29, 2021

# Sun heated MeV-scale dark matter and the XENON1T electron recoil excess

**Yifan Chen,**[a] **Ming-Yang Cui,**[b] **Jing Shu,**[a,c,d,e,f,g] **Xiao Xue,**[a,c] **Guan-Wen Yuan**[b,h] **and Qiang Yuan**[b,f,h]

[a] *CAS Key Laboratory of Theoretical Physics, Insitute of Theoretical Physics, Chinese Academy of Sciences, Beijing 100190, China*
[b] *Key Laboratory of Dark Matter and Space Astronomy, Purple Mountain Observatory, Chinese Academy of Sciences, Nanjing 210023, China*
[c] *School of Physical Sciences, University of Chinese Academy of Sciences, Beijing 100049, China*
[d] *CAS Center for Excellence in Particle Physics, Beijing 100049, China*
[e] *School of Fundamental Physics and Mathematical Sciences, Hangzhou Institute for Advanced Study, University of Chinese Academy of Sciences, Hangzhou 310024, China*
[f] *Center for High Energy Physics, Peking University, Beijing 100871, China*
[g] *International Center for Theoretical Physics Asia-Pacific, Beijing/Hanzhou, China*
[h] *School of Astronomy and Space Science, University of Science and Technology of China, Hefei 230026, China*

*E-mail:* yifan.chen@itp.ac.cn, mycui@pmo.ac.cn, jshu@itp.ac.cn, xuexiao@itp.ac.cn, yuangw@pmo.ac.cn, yuanq@pmo.ac.cn

Abstract: The XENON1T collaboration reported an excess of the low-energy electron recoil events between 1 and 7 keV. We explore the possibility to explain such an anomaly by the MeV-scale dark matter (DM) heated by the interior of the Sun due to the same DM-electron interaction as in the detector. The kinetic energies of heated DM particles can reach a few keV, and can potentially account for the excess signals detected by XENON1T. We study different form factors of the DM-electron interactions, $F(q) \propto q^i$ with $q$ being the momentum exchange and $i = 0, 1, 2$, and find that for all these cases the inclusion of the Sun-heated DM component improves the fit to the XENON1T data. The inferred DM-electron scattering cross section (at $q = \alpha m_e$ where $\alpha$ is the fine structure constant and $m_e$ is electron mass) is from $\sim 10^{-38}\,\mathrm{cm}^2$ (for $i = 0$) to $\sim 10^{-42}\,\mathrm{cm}^2$ (for $i = 2$). We also derive constraints on the DM-electron cross sections for these form factors, which are stronger than previous results with similar assumptions. We emphasize that the Sun-heated DM scenario relies on the minimum assumption on DM models, which serves as a general explanation of the XENON1T anomaly via DM-electron interaction. The spectrum of the



https://doi.org/10.1007/JHEP04(2021)282

Sun-heated DM is typically soft comparing to other boosted DM, so the small recoil events are expected to be abundant in this scenario. More sensitive direct detection experiments with lower thresholds can possibly distinguish this scenario with other boosted DM models or solar axion models.

Keywords: Beyond Standard Model, Cosmology of Theories beyond the SM

ArXiv ePrint: 2006.12447

JHEP04(2021)282

## Contents



JHEP04(2021)282

## 1 Introduction

The direct detection of dark matter (DM) has reached unprecedented sensitivities. Nevertheless, no convincing signals have been detected yet (see e.g., [1, 2]). Very recently, the XENON1T collaboration reported a potential excess of electron recoils in the range of 1–7 keV above the known backgrounds [3]. The total number of events in such a recoil energy window is 285, while the expected background number is $232 \pm 15$, which suggests a significance of $3.5\sigma$. Although the unknown backgrounds from tritium decay cannot be reliably ruled out, the estimated tritium concentration is much lower than that required to fit the data [3]. The subsequent search for similar signals with the PandaX-II data gave constraints which were consistent with the XENON1T result, although no significant signal was detected in Pandax-II [4]. It has been postulated that the hypothetical effects from e.g., solar axions [5, 6] or the neutrino magnetic moment [7, 8] can account for the XENON1T data. However, the required model parameters are found to be in conflict with other constraints, particularly the astrophysical observations [9–13] (see however, [14]). Alternatively, several attempts [15–22] have been proposed to explain the XENON1T data.

While the traditional weakly interacting massive particles in the Galactic halo are difficult to account for the XENON1T excess due to the very low energy deposits when scattering with electrons, one class of models with DM being boosted to relatively high velocities ($\sim 0.1c$) can potentially work [17, 18]. In ref. [17] a fast DM component is simply assumed, and the possible mechanisms to produce such fast DM have been discussed, including e.g., a fast-moving subhalo, semi-annihilating DM, or nearby axion stars. A realization of the boosted DM scenario has been given in ref. [18], where a faster DM component from the semi-annihilation of DM in the Galactic center has been proposed. The Sun could also be a site to accumulate enough DM in its interior via the DM-nucleon or DM-electron scattering. However, in this case, the required cross section is too high that the Sun would be opaque for the DM to escape [18].

The high-temperature plasma inside the Sun can be a natural source to heat up light DM particles [23]. The temperature of the interior of the Sun is about $1.5 \times 10^7$ K. As long as the scattering between DM and the electrons is moderately efficient (for example,

the scattering cross section $\sim$ pb), the DM can be heated up to energies of $\sim$keV and can potentially account for the XENON1T excess. Comparing with other boosted DM models (e.g., those discussed in [17, 18]), this scenario is quite clear and simple: the DM-electron scattering as seen in the detector occurs inevitably in the Sun (or any other places with material). This model gives a natural boost of DM, without additional assumptions (e.g., the high-speed DM subhalos [17], and the semi-annihilation/multi-component DM [18]). In particular, the heated DM from the Sun could be a unique signal for future tests with directional direct detection experiments.

## 2 Dark matter heated by the Sun

The heated DM flux observed on the Earth can be estimated as [23]

$$\Phi_{\rm heat} \sim \frac{\Phi_{\rm halo} S_g}{4\pi d^2} \times \begin{cases} \dfrac{4\pi R_{\rm core}^3}{3\lambda}, & R_{\rm core} \ll \lambda \\ \pi R_{\rm scatt}^2, & R_{\rm core} \gg \lambda \end{cases}, \tag{2.1}$$

where $\Phi_{\rm halo}$ is the DM flux in the local Milky Way halo, $R_{\rm core} \sim 0.2 R_\odot$ is the core radius of the Sun, $d \equiv 1.5\times10^{13}$ cm is the Sun-Earth distance, $S_g$ describes the gravitational focusing effect which enhances the scatterings, $R_{\rm scatt}$ is the characteristic scattering radius at which the DM-electron scattering once on average, $\lambda$ is the mean free path of a DM particle inside the core of the Sun. For weak scattering limit, the mean free path is large, and the scattering probability is proportional to the volume of the Sun's core, which is $4\pi R_{\rm core}^3/3$. On the other hand, if the scattering is frequent, the scattering probability is proportional to the characteristic scattering area $\pi R_{\rm scatt}^2$. Note that if interaction is strong enough, $R_{\rm scatt}$ reaches a maximum of $R_\odot$, and the heated DM fluxes become weakly dependent of the scattering cross section. The factor $S_g$ is estimated to be $\mathcal{O}(10)$ according to the ratio of the escape velocity of the Sun and the halo DM velocity [23].

More accurately, the differential scattering cross section between a DM particle and an electron can be written as

$$\frac{d\sigma}{d\cos\theta\, d\phi} = \frac{\bar{\sigma}_{\rm e}}{4\pi} |F(q)|^2, \tag{2.2}$$

where $\theta$ and $\phi$ represent the spherical coordinate angles of the final state in the center-of-mass frame of each scattering. $\bar{\sigma}_e \equiv \dfrac{\mu^2 \overline{\left|\mathcal{M}_{\rm free}\,(\alpha m_e)\right|^2}}{16\pi m_{\rm dm}^2 m_{\rm e}^2}$ is the reference electron-DM cross section evaluated at $q = \alpha m_{\rm e}$, in which $m_{\rm e}$ and $m_{\rm dm}$ are the masses of electron and DM and $\mu$ is the reduced mass of the two. $F(q)$ is the DM form factor depending on the momentum transfer $q$. In the center-of-mass frame, $F(q)$ represents a weight of angle between the initial and final states. In this work, we consider three examples of form factors: $F = 1$, $F = \frac{q}{\alpha m_{\rm e}}$ and $F = (\frac{q}{\alpha m_{\rm e}})^2$. These operators all originate from a heavy mediator whose mass is much heavier than the typical momentum transfer. The latter two $q$-dependent form factors can be derived, for example, from dimension six operators with scalar-pseudoscalar interaction $\bar{\chi}\gamma_5\chi\bar{e}e$ and pseudoscalar-pseudoscalar interaction $\bar{\chi}\gamma_5\chi\bar{e}\gamma_5 e$, respectively [24].



JHEP04(2021)282

To properly handle the multiple scatterings, Monte Carlo simulations are usually required to calculate the energy distribution and fluxes of DM reflected by the Sun. Following ref. [23], we do such simulations taking into account the updated standard solar model [25]. We start the simulation through generating halo DM particles with a truncated Maxwell distribution, with the most probable velocity of 220 km s$^{-1}$ and an escape velocity of 540 km s$^{-1}$. The impact parameter with respect to the Sun is adopted to be $4R_\odot$. The gravitational bending of the DM particle outside the Sun is computed with the Newton's law. When the DM enters the Sun, the gravitational effect is neglected, and only the scattering with electrons are considered. The interior of the Sun is approximated to be electron-ion plasma, and the electron number density is calculated according to the radius-dependent composition model of the Sun [25]. A mean free path of a DM particle is calculated as $\lambda(r) = v_{\rm dm}(r)/[n_e(r)\langle\sigma_e v_r\rangle]$ [23], which is a function of radius $r$ inside the Sun. In the above formula, $v_{\rm dm}(r)$ is the DM velocity, and $v_r$ is the relative velocity between DM and electrons. The calculation of the mean free path considers the fact that the thermal electrons move with a very high speed, but do not travel far in the Sun. The interaction probability of the DM particle is $P = 1 - e^{-l_{\rm step}/\lambda}$ after traveling a distance of one step $l_{\rm step}$. When the DM particle leaves the Sun, a gravitational redshift of the particle energy with $E_{\rm final} = E_{\rm surf} - m_{\rm dm}v_{\rm esc}^2/2$ is applied, where $E_{\rm surf}$ is the DM kinetic energy at the Sun's surface and $E_{\rm final}$ is its final kinetic energy escaping from the Sun. For those DM particles that do not hit the Sun, their kinetic energies keep unchanged as the initial values. The heated DM flux is then [23]

$$\frac{d\Phi_{\rm heat}}{dE_{\rm dm}} = \Phi_{\rm halo} \times \frac{16\pi R_\odot^2 F(E_{\rm dm})}{4\pi d^2}, \tag{2.3}$$

where $F(E_{\rm dm})$ is the normalized kinetic energy distribution of DM with the reflection of the Sun, and $16\pi R_\odot^2$ is the impact area adopted in the simulation.

The energy spectrum of the heated DM depends on the DM mass and the scattering cross section [23]. Since most of the heated DM particles have kinetic energies lower than the threshold of the current XENON1T analysis ($\sim 1$ keV), we expect that only the high-energy tail would contribute to the XENON1T events. For a 2-body elastic scattering with the electron at rest, the maximum recoil energy is

$$E_{\rm r}^{\rm max} = \frac{4E_{\rm dm}m_{\rm e}m_{\rm dm}}{(m_{\rm e}+m_{\rm dm})^2} > 1 \text{ keV}, \tag{2.4}$$

where $E_{\rm dm}$ is the kinetic energy of the DM. The energy transfer in both the scatterings inside the Sun and in the detector is the most efficient if $m_{\rm dm} \sim m_{\rm e}$.

Figure 1 shows the normalized DM energy spectrum after the scattering with the Sun, for the three types of DM form factors. For each form factor, we choose the DM mass and cross section which best-fit the XENON1T data (see below section 3). As expected, the higher power of $q$ of the form factor leads to a harder spectrum.



JHEP04(2021)282

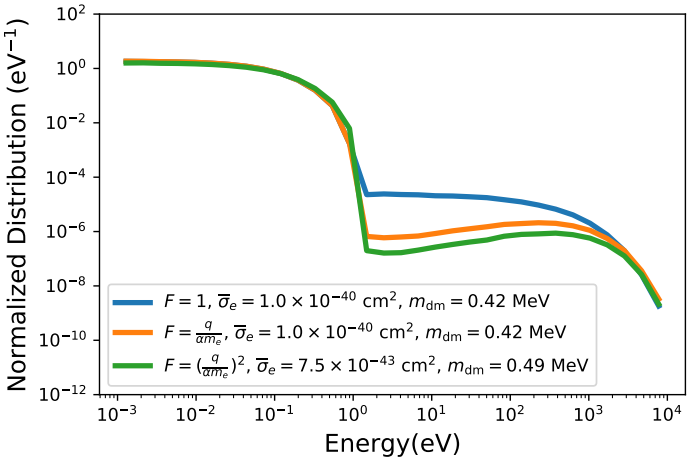


**Figure 1**. Normalized energy distributions of the heated DM fluxes on the Earth for parameters given in eq. (3.3), for $F = 1$, $F = \frac{q}{\alpha m_e}$, and $F = (\frac{q}{\alpha m_e})^2$, respectively.

## 3 Confronting the new XENON1T data

To compare with the XENON1T data, we calculate the event rate of electron recoils in the detector as

$$\frac{\mathrm{d}N}{\mathrm{d}E_{\rm r}} = N_d \times \int \frac{\mathrm{d}\sigma}{\mathrm{d}E_{\rm r}}(v_{\rm dm}, E_{\rm r}) \frac{\mathrm{d}\Phi_{\rm heat}}{\mathrm{d}v_{\rm dm}} \mathrm{d}v_{\rm dm}, \tag{3.1}$$

where $N_d \simeq 4.2 \times 10^{27}$ ton$^{-1}$ is the number of Xe atoms for one ton mass of the detector, $v_{\rm dm}$ is the velocity of the DM particle, $E_{\rm r}$ is the electron recoil energy, $\mathrm{d}\sigma/\mathrm{d}E_{\rm r}$ is the differential scattering cross section, and $\mathrm{d}\Phi_{\rm heat}/\mathrm{d}v_{\rm dm}$ is the spectrum of the heated DM component.

Following refs. [26–28], the differential cross section for fixed DM velocity can be written as

$$\frac{\mathrm{d}\sigma}{\mathrm{d}E_{\rm r}}(v_{\rm dm}, E_{\rm r}) = \frac{\bar{\sigma}_{\rm e} m_{\rm e}}{2\mu^2 v_{\rm dm}^2} \int_{q_-}^{q_+} a_0^2 \, q \, \mathrm{d}q \, |F(q)|^2 \, K(E_{\rm r}, q), \tag{3.2}$$

where $a_0 = 1/(\alpha m_{\rm e})$ is the Bohr radius, and the integration limits are $q_\pm = m_{\rm dm} v_{\rm dm} \pm \sqrt{m_{\rm dm}^2 v_{\rm dm}^2 - 2 m_{\rm dm} E_{\rm r}}$. The atomic excitation factor $K(E_{\rm r}, q)$, describing the probability of obtaining a particular recoil energy for an ionized electron given momentum transfer $q$, is taken from refs. [29, 30] where the initial bound states contain Roothan-Hartree-Fock (RHF) wave functions with the coefficients being tabulated in ref. [31] and the final state wave functions given in ref. [32]. $K(E_{\rm r}, q)$ is related to the atomic response function in ref. [29] through $K(E_{\rm r}, q) = \sum_{n\ell} \frac{\left|f_{\rm ion}^{n\ell}(k', q)\right|^2}{2k'^2 a_0^2} \theta(E_{\rm r} - E_b^{n\ell})$, where $E_{\rm r} = E_b^{n\ell} + k'^2/2m_{\rm e}$, $E_b^{n\ell}$ is the minus binding energy of the initial state electron, and $k'$ is the momentum of the final state ionized electron. We consider the contributions from all accessible atomic energy states of Xe.

We further convolve the event rate with a Gaussian energy resolution function with a width of $\sigma(E) = 0.310\sqrt{\rm keV}\sqrt{E} + 0.0037E$ and multiply the detection efficiency as given in ref. [3]. The best-fit results of the event rate distributions are shown in the left panels



JHEP04(2021)282

figure 2, for the three form factors adopted here. The best-fit model parameters and (logarithmic) likelihood ratios are

$$\begin{aligned}
&m_{\rm dm}=0.42\ {\rm MeV},\quad \bar{\sigma}_{\rm e}=1.0\times10^{-38}\ {\rm cm}^2,\quad 2\ln(\mathcal{L}_{S+B}/\mathcal{L}_B)=4.8,\quad F=1;\\
&m_{\rm dm}=0.42\ {\rm MeV},\quad \bar{\sigma}_{\rm e}=1.0\times10^{-40}\ {\rm cm}^2,\quad 2\ln(\mathcal{L}_{S+B}/\mathcal{L}_B)=9.3,\quad F=\frac{q}{\alpha m_{\rm e}};\\
&m_{\rm dm}=0.49\ {\rm MeV},\quad \bar{\sigma}_{\rm e}=7.5\times10^{-43}\ {\rm cm}^2,\quad 2\ln(\mathcal{L}_{S+B}/\mathcal{L}_B)=12.1,\quad F=\left(\frac{q}{\alpha m_{\rm e}}\right)^2. \qquad (3.3)
\end{aligned}$$

In the above equation the likelihood function is defined as the Poisson likelihood $\mathcal{L}=\prod_{i=1}^{7}e^{-\mu_i}\mu_i^{n_i}/n_i!$, where $i$ denotes the $i$th energy bin, $n_i$ is the number of detected events, and $\mu_i$ is the expected number of events from the model. $S+B$ means the signal+background model and $B$ means the background-only model. In this work the first 7 bins of the XENON1T data are considered. The logarithmic likelihood ratios of the fits give significance of the Sun-heated DM of $1.7\,\sigma$, $2.6\,\sigma$, and $3.0\,\sigma$, for $F(q)=1$, $\frac{q}{\alpha m_{\rm e}}$, and $(\frac{q}{\alpha m_{\rm e}})^2$, respectively, for 2 additional degrees of freedom.

As can be seen, for $F(q)=1$, the improvement of the fit compared with the background hypothesis is not significant, due to the very soft energy spectrum of the Sun-heated DM. The results for $F=\frac{q}{\alpha m_{\rm e}}$ and $F=(\frac{q}{\alpha m_{\rm e}})^2$ are much better. This is expected, since the XENON1T data requires a relatively hard spectrum of the recoil events (the background expectation is consistent with the data in the first bin from 1 to 2 keV) and hence the DM spectrum. We further see that the best-fit values of the DM mass is indeed close to $m_e$, with a slight dependence on the form factor.

In the right panels of figure 2 we show the distributions of $-2\Delta\ln\mathcal{L}=-2\ln(\mathcal{L}_{S+B}/\mathcal{L}_B)$ on the $m_{\rm dm}-\bar{\sigma}_{\rm e}$ plane. A negative value of $-2\Delta\ln\mathcal{L}$ means a favor of the model by the data. To be conservative, we also derive the 95% upper bounds on the DM-electron cross section $\bar{\sigma}_{\rm e}$, via requiring $-2\Delta\ln\mathcal{L}=-2\ln(\mathcal{L}_{S+B}/\mathcal{L}^{\rm max}_{S+B})=2.71$, for each fixed $m_{\rm dm}$. If a signal is indicated by the data, we start the scan of $\bar{\sigma}_{\rm e}$ from the best-fit value to the larger side to derive the constraints. The 95% exclusion limits are shown by the black dashed lines in the right panels of figure 2. For the case of $F(q)=1$, our results using the XENON1T 2020 data are more stringent than that of ref. [23] which considered the same Sun-heated DM model but with XENON1T 2017 data. Compared with the results from the low-threshold SENSEI experiment [33], considering the DM scattering in the Sun can also effectively extend the sensitive range to lower DM masses.

For a given UV-completed model to realize the form factors, one requires the cutoff scale to be large enough to avoid the constraints from collider results [36]. For $F=\frac{q}{\alpha m_{\rm e}}$, a dimension five operator $\phi^*\phi\bar{e}\gamma_5 e$ representing the interaction between scalar DM and electron spin, is discussed in [24] for $m_{\rm DM}\simeq100\,{\rm GeV}$ where the cutoff scale can be hundreds of GeV that is consistent with both collider and electron Electric Dipole Moment (EDM) constraints. In our case, the lower dark matter mass can lead to an even larger cutoff around $10^6\,{\rm GeV}$ [24]. On the other hand, for $F=(\frac{q}{\alpha m_{\rm e}})^2$, if one takes the dimension six operator $\bar{\chi}\gamma_5\chi\bar{e}\gamma_5 e$, the cutoff scale is always lower than 1 GeV for the parameters in eq. (3.3), which requires a more sophisticated model building to avoid the collider constraints.



JHEP04(2021)282

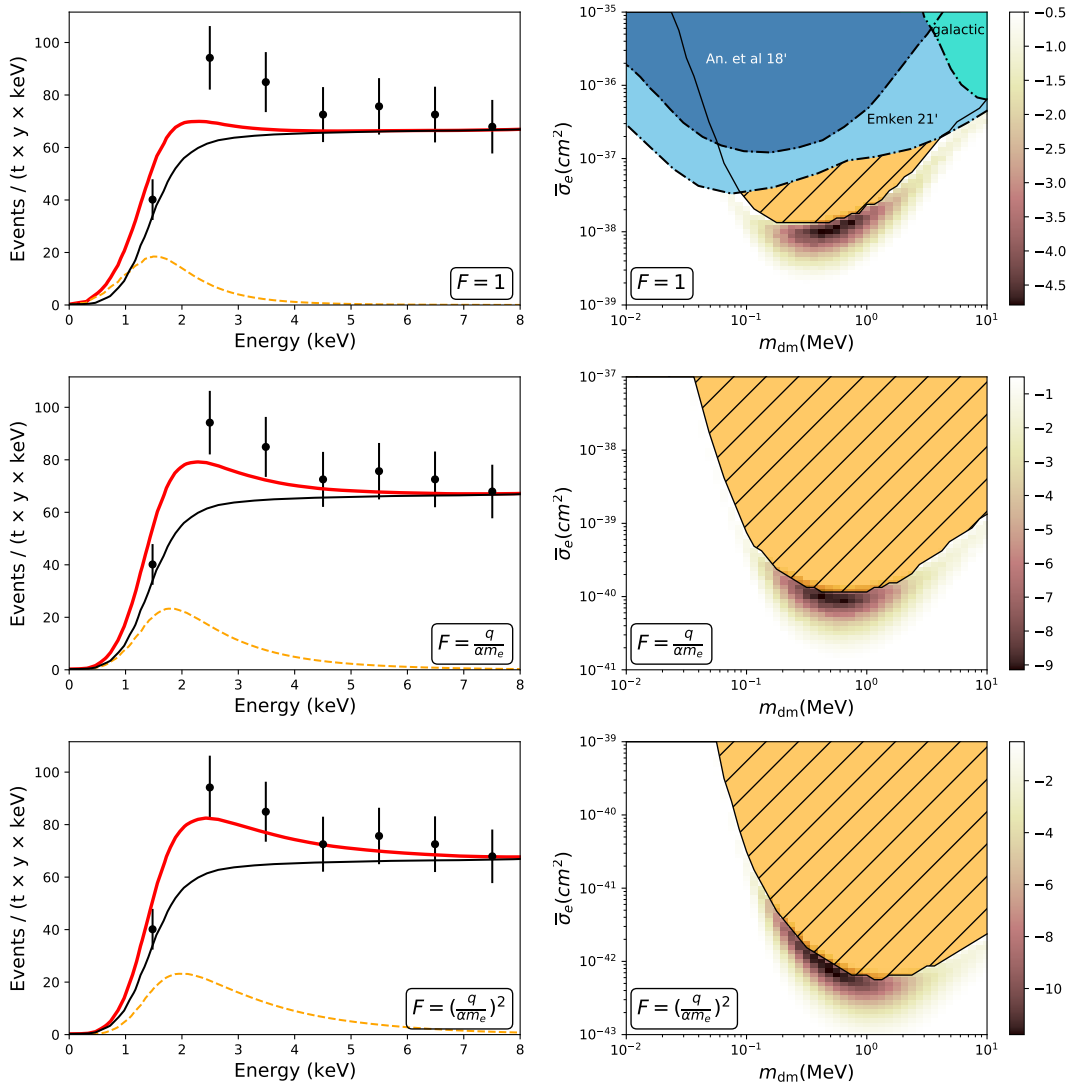


**Figure 2**. Left: best-fit results to the XENON1T data when the Sun-heated DM-induced electron recoils are included, for $F(q) = 1$ (top), $\frac{q}{\alpha m_e}$ (middle), and $(\frac{q}{\alpha m_e})^2$ (bottom), respectively. See the text for the best-fit model parameters. Right: 95% exclusion regions (hatched orange areas) on the $m_{\rm dm} - \bar{\sigma}_{\rm e}$ plane from the XENON1T 2020 data. For the $F(q) = 1$ case, previous limits from ref. [23] considering the Sun-heated DM scenario and the recent bounds from low-threshold SENSEI experiment [33] are also shown for comparison, as well as a bound based on the S2-only analysis [34, 35].

We note also that there are cosmological and astrophysical bounds on the DM-electron interactions, such as BBN, CMB, the overproduction of DM [37], and the supernova cooling [38, 39]. These bounds are based on heavy mediator assumption with mass much higher than the typical energy scale around 10 MeV. Discussion on DM coupled through lighter mediators with form factor $F = 1$ were summarized in [40], where the HB stars exclude the mediator mass below 0.1 MeV. Since the momentum exchange of the dominant scatterings considered in this work is relatively small ($\sim$keV), we expect that there is a viable mass



JHEP04(2021)282

range of the mediator which is heavy enough that the contact interaction assumption in this work holds but is smaller than that required when the cosmological and supernova bounds apply. A late phase transition in the dark sector may modify the thermal history and relax the cosmological constraint as well (e.g., [41–43]).

## 4 Conclusion and discussion

In this work we show that the electron recoil event excess detected by XENON1T [3] can be explained by MeV-scale DM particles interacting with electrons in the detector. While the slow (with velocity $\sim 10^{-3}c$) DM particles in the Milky Way halo can not give electron recoils with energies of keV, the Sun plays a key role in heating a fraction of DM particles just to keV energies, leaving detectable signals in the detector. The goodness-of-fit depends on the assumed form factor of the DM-electron scattering. For $F(q) \propto q^i$ ($i > 0$), the model can fit the data reasonably well. The best-fit DM mass is close to $m_e$, and the scattering cross section $\bar{\sigma}_{\rm e}$ is about $10^{-38}\,{\rm cm}^2$ (for $i = 0$), $10^{-40}\,{\rm cm}^2$ (for $i = 1$), and $10^{-42}\,{\rm cm}^2$ (for $i = 2$). For $i = 0$ and 1, these parameters can be consistent with other constraints (e.g., [44, 45]). However, for a strong $q$-dependence, other observations at higher energy scales may constrain the model. We emphasize that the physical process occurs in the Sun is the same as that in the detector, and thus no additional assumption is needed other than the DM-electron scattering. To be conservative, we also derive upper limits of the reference cross section $\bar{\sigma}_{\rm e}$ between DM and electrons, for these different form factors. Note that for $i = 1$ and 2, these constraints are presented for the first time. For $i = 0$, our constraints are also stronger than previous works [23, 33].

Compared with other boosted DM models [17, 18], the Sun-heated DM has a softer energy spectrum which would result in quite a few low-recoil-energy events. A rough estimate of the number of events due to the Sun-heated DM according to the best-fit model parameters in eq. (3.3) gives consistent results with the XENON1T S2-only data [35]. Similar result was also shown recently in [34]. Future direct detection experiments with lower thresholds or higher low-energy efficiencies would be able to distinguish this scenario from others. Furthermore, the direction sensitive direct detection experiments [46] may also directly test this model, with the Sun being the main source of such heated DM.

Cosmic rays in the Milky Way could also boost DM particles to high (or even very high) energies [47–49]. As already commented in ref. [17], the cosmic ray electron boosted DM model seems to give conflicted results with that of neutrino experiments, since the neutrino experiments are more sensitive than the direct detection experiments for those electron boosted DM [44]. For the scenario that DM particles are boosted by cosmic ray nuclei, which then interact with electrons in the detector, the boosted DM fluxes seems to be also too low to be consistent with the existing constraints. For example, taking $F(q) = 1$ and $\sigma_{\chi p} \sim 10^{-31}\,{\rm cm}^2$ as an illustration, the peak flux of the boosted DM is about $10^{-6}\,{\rm cm}^{-2}\,{\rm s}^{-1}$ [48, 50]. For such a DM flux, the required cross section to account for the XENON1T excess events is $\mathcal{O}(10^{-28})$ cm$^2$ [18], which exceeds significantly the current limits by neutrino experiments [44].



JHEP04(2021)282

## Acknowledgments

We thank Shao-Feng Ge and Yue Zhao for helpful discussion. Y.C. is supported by the China Postdoctoral Science Foundation under Grant No. 2020T130661, No. 2020M680688, the International Postdoctoral Exchange Fellowship Program, and by the National Natural Science Foundation of China (NSFC) under Grants No. 12047557. J.S. is supported by the National Natural Science Foundation of China under Grants No. 12025507, No. 11690022, No.11947302; and is supported by the Strategic Priority Research Program and Key Research Program of Frontier Science of the Chinese Academy of Sciences under Grants No. XDB21010200, No. XDB23010000, and No. ZDBS-LY-7003. Q.Y. is supported by the NSFC under Grants No. 11722328, No. 11851305, the 100 Talents program of Chinese Academy of Sciences, and the Program for Innovative Talents and Entrepreneur in Jiangsu. We acknowledge the use of HPC Cluster of ITP-CAS.



## References

[1] J. Liu, X. Chen and X. Ji, *Current status of direct dark matter detection experiments*, *Nature Phys.* **13** (2017) 212 [arXiv:1709.00688] [INSPIRE].

[2] M. Schumann, *Direct Detection of WIMP Dark Matter: Concepts and Status*, *J. Phys. G* **46** (2019) 103003 [arXiv:1903.03026] [INSPIRE].

[3] XENON collaboration, *Excess electronic recoil events in XENON1T*, *Phys. Rev. D* **102** (2020) 072004 [arXiv:2006.09721] [INSPIRE].

[4] PandaX-II collaboration, *A search for solar axions and anomalous neutrino magnetic moment with the complete PandaX-II data*, arXiv:2008.06485 [INSPIRE].

[5] J. Redondo, *Solar axion flux from the axion-electron coupling*, *JCAP* **12** (2013) 008 [arXiv:1310.0823] [INSPIRE].

[6] S. Moriyama, *A Proposal to search for a monochromatic component of solar axions using Fe-57*, *Phys. Rev. Lett.* **75** (1995) 3222 [hep-ph/9504318] [INSPIRE].

[7] N.F. Bell, V. Cirigliano, M.J. Ramsey-Musolf, P. Vogel and M.B. Wise, *How magnetic is the Dirac neutrino?*, *Phys. Rev. Lett.* **95** (2005) 151802 [hep-ph/0504134] [INSPIRE].

[8] N.F. Bell, M. Gorchtein, M.J. Ramsey-Musolf, P. Vogel and P. Wang, *Model independent bounds on magnetic moments of Majorana neutrinos*, *Phys. Lett. B* **642** (2006) 377 [hep-ph/0606248] [INSPIRE].

[9] N. Viaux et al., *Neutrino and axion bounds from the globular cluster M5 (NGC 5904)*, *Phys. Rev. Lett.* **111** (2013) 231301 [arXiv:1311.1669] [INSPIRE].

[10] A. Ayala, I. Domínguez, M. Giannotti, A. Mirizzi and O. Straniero, *Revisiting the bound on axion-photon coupling from Globular Clusters*, *Phys. Rev. Lett.* **113** (2014) 191302 [arXiv:1406.6053] [INSPIRE].



JHEP04(2021)282

[11] M. Giannotti, I.G. Irastorza, J. Redondo, A. Ringwald and K. Saikawa, *Stellar Recipes for Axion Hunters*, *JCAP* **10** (2017) 010 [arXiv:1708.02111] [INSPIRE].

[12] A.H. Córsico, L.G. Althaus, M.M. Miller Bertolami, S.O. Kepler and E. García-Berro, *Constraining the neutrino magnetic dipole moment from white dwarf pulsations*, *JCAP* **08** (2014) 054 [arXiv:1406.6034] [INSPIRE].

[13] S.A. Díaz, K.-P. Schröder, K. Zuber, D. Jack and E.E.B. Barrios, *Constraint on the axion-electron coupling constant and the neutrino magnetic dipole moment by using the tip-RGB luminosity of fifty globular clusters*, arXiv:1910.10568 [INSPIRE].

[14] C. Gao, J. Liu, L.-T. Wang, X.-P. Wang, W. Xue and Y.-M. Zhong, *Reexamining the Solar Axion Explanation for the XENON1T Excess*, *Phys. Rev. Lett.* **125** (2020) 131806 [arXiv:2006.14598] [INSPIRE].

[15] J. Smirnov and J.F. Beacom, *New Freezeout Mechanism for Strongly Interacting Dark Matter*, *Phys. Rev. Lett.* **125** (2020) 131301 [arXiv:2002.04038] [INSPIRE].

[16] F. Takahashi, M. Yamada and W. Yin, *XENON1T Excess from Anomaly-Free Axionlike Dark Matter and Its Implications for Stellar Cooling Anomaly*, *Phys. Rev. Lett.* **125** (2020) 161801 [arXiv:2006.10035] [INSPIRE].

[17] K. Kannike, M. Raidal, H. Veermäe, A. Strumia and D. Teresi, *Dark Matter and the XENON1T electron recoil excess*, *Phys. Rev. D* **102** (2020) 095002 [arXiv:2006.10735] [INSPIRE].

[18] B. Fornal, P. Sandick, J. Shu, M. Su and Y. Zhao, *Boosted Dark Matter Interpretation of the XENON1T Excess*, *Phys. Rev. Lett.* **125** (2020) 161804 [arXiv:2006.11264] [INSPIRE].

[19] G. Alonso-Álvarez, F. Ertas, J. Jaeckel, F. Kahlhoefer and L.J. Thormaehlen, *Hidden Photon Dark Matter in the Light of XENON1T and Stellar Cooling*, *JCAP* **11** (2020) 029 [arXiv:2006.11243] [INSPIRE].

[20] C. Boehm, D.G. Cerdeno, M. Fairbairn, P.A.N. Machado and A.C. Vincent, *Light new physics in XENON1T*, *Phys. Rev. D* **102** (2020) 115013 [arXiv:2006.11250] [INSPIRE].

[21] L. Su, W. Wang, L. Wu, J.M. Yang and B. Zhu, *Atmospheric Dark Matter and Xenon1T Excess*, *Phys. Rev. D* **102** (2020) 115028 [arXiv:2006.11837] [INSPIRE].

[22] M. Du, J. Liang, Z. Liu, V.Q. Tran and Y. Xue, *On-shell mediator dark matter models and the Xenon1T excess*, *Chin. Phys. C* **45** (2021) 013114 [arXiv:2006.11949] [INSPIRE].

[23] H. An, M. Pospelov, J. Pradler and A. Ritz, *Directly Detecting MeV-scale Dark Matter via Solar Reflection*, *Phys. Rev. Lett.* **120** (2018) 141801 [*Erratum ibid.* **121** (2018) 259903] [arXiv:1708.03642] [INSPIRE].

[24] I.M. Bloch, A. Caputo, R. Essig, D. Redigolo, M. Sholapurkar and T. Volansky, *Exploring new physics with O(keV) electron recoils in direct detection experiments*, *JHEP* **01** (2021) 178 [arXiv:2006.14521] [INSPIRE].

[25] N. Vinyoles et al., *A new Generation of Standard Solar Models*, *Astrophys. J.* **835** (2017) 202 [arXiv:1611.09867] [INSPIRE].

[26] R. Essig, A. Manalaysay, J. Mardon, P. Sorensen and T. Volansky, *First Direct Detection Limits on sub-GeV Dark Matter from XENON10*, *Phys. Rev. Lett.* **109** (2012) 021301 [arXiv:1206.2644] [INSPIRE].



JHEP04(2021)282

[27] B.M. Roberts, V.A. Dzuba, V.V. Flambaum, M. Pospelov and Y.V. Stadnik, *Dark matter scattering on electrons: Accurate calculations of atomic excitations and implications for the DAMA signal*, *Phys. Rev. D* **93** (2016) 115037 [arXiv:1604.04559] [INSPIRE].

[28] B.M. Roberts and V.V. Flambaum, *Electron-interacting dark matter: Implications from DAMA/LIBRA-phase2 and prospects for liquid xenon detectors and NaI detectors*, *Phys. Rev. D* **100** (2019) 063017 [arXiv:1904.07127] [INSPIRE].

[29] R. Catena, T. Emken, N.A. Spaldin and W. Tarantino, *Atomic responses to general dark matter-electron interactions*, *Phys. Rev. Res.* **2** (2020) 033195 [arXiv:1912.08204] [INSPIRE].

[30] T. Emken, *Dark Matter-induced Atomic Response Code (DarkARC) v1.0*, (2019) https://github.com/temken/DarkARC [10.5281/zenodo.3581334].

[31] C.F. Bunge, J.A. Barrientos, A.V. Bunge, *Roothaan-Hartree-Fock Ground-State Atomic Wave Functions: Slater-Type Orbital Expansions and Expectation Values for $Z = 2$–54*, *Atom. Data Nucl. Data Tabl.* **53** (1993) 113.

[32] H.A. Bethe and E.E. Salpeter, *Quantum Mechanics of One- and Two-Electron Atoms*, Springer US (1957) [DOI].

[33] SENSEI collaboration, *SENSEI: Direct-Detection Results on sub-GeV Dark Matter from a New Skipper-CCD*, *Phys. Rev. Lett.* **125** (2020) 171802 [arXiv:2004.11378] [INSPIRE].

[34] T. Emken, *Solar reflection of light dark matter with heavy mediators*, arXiv:2102.12483 [INSPIRE].

[35] XENON collaboration, *Light Dark Matter Search with Ionization Signals in XENON1T*, *Phys. Rev. Lett.* **123** (2019) 251801 [arXiv:1907.11485] [INSPIRE].

[36] P.J. Fox, R. Harnik, J. Kopp and Y. Tsai, *LEP Shines Light on Dark Matter*, *Phys. Rev. D* **84** (2011) 014028 [arXiv:1103.0240] [INSPIRE].

[37] B.V. Lehmann and S. Profumo, *Cosmology and prospects for sub-MeV dark matter in electron recoil experiments*, *Phys. Rev. D* **102** (2020) 023038 [arXiv:2002.07809] [INSPIRE].

[38] W. DeRocco, P.W. Graham, D. Kasen, G. Marques-Tavares and S. Rajendran, *Supernova signals of light dark matter*, *Phys. Rev. D* **100** (2019) 075018 [arXiv:1905.09284] [INSPIRE].

[39] S. Chigusa, M. Endo and K. Kohri, *Constraints on electron-scattering interpretation of XENON1T excess*, *JCAP* **10** (2020) 035 [arXiv:2007.01663] [INSPIRE].

[40] S. Knapen, T. Lin and K.M. Zurek, *Light Dark Matter: Models and Constraints*, *Phys. Rev. D* **96** (2017) 115021 [arXiv:1709.07882] [INSPIRE].

[41] Z. Chacko, L.J. Hall, S.J. Oliver and M. Perelstein, *Late time neutrino masses, the LSND experiment and the cosmic microwave background*, *Phys. Rev. Lett.* **94** (2005) 111801 [hep-ph/0405067] [INSPIRE].

[42] H. Davoudiasl and C.W. Murphy, *Fuzzy Dark Matter from Infrared Confining Dynamics*, *Phys. Rev. Lett.* **118** (2017) 141801 [arXiv:1701.01136] [INSPIRE].

[43] Y. Zhao, *Cosmology and time dependent parameters induced by a misaligned light scalar*, *Phys. Rev. D* **95** (2017) 115002 [arXiv:1701.02735] [INSPIRE].

[44] Y. Ema, F. Sala and R. Sato, *Light Dark Matter at Neutrino Experiments*, *Phys. Rev. Lett.* **122** (2019) 181802 [arXiv:1811.00520] [INSPIRE].

[45] C. Cappiello and J.F. Beacom, *Strong New Limits on Light Dark Matter from Neutrino Experiments*, *Phys. Rev. D* **100** (2019) 103011 [arXiv:1906.11283] [INSPIRE].



JHEP04(2021)282

[46] F. Mayet et al., *A review of the discovery reach of directional Dark Matter detection*, *Phys. Rept.* **627** (2016) 1 [arXiv:1602.03781] [INSPIRE].

[47] C.V. Cappiello, K.C.Y. Ng and J.F. Beacom, *Reverse Direct Detection: Cosmic Ray Scattering With Light Dark Matter*, *Phys. Rev. D* **99** (2019) 063004 [arXiv:1810.07705] [INSPIRE].

[48] T. Bringmann and M. Pospelov, *Novel direct detection constraints on light dark matter*, *Phys. Rev. Lett.* **122** (2019) 171801 [arXiv:1810.10543] [INSPIRE].

[49] W. Yin, *Highly-boosted dark matter and cutoff for cosmic-ray neutrinos through neutrino portal*, *EPJ Web Conf.* **208** (2019) 04003 [arXiv:1809.08610] [INSPIRE].

[50] S.-F. Ge, J. Liu, Q. Yuan and N. Zhou, *Diurnal Effect of Sub-GeV Dark Matter Boosted by Cosmic Rays*, *Phys. Rev. Lett.* **126** (2021) 091804 [arXiv:2005.09480] [INSPIRE].

JHEP04(2021)282